DART

NASA

Dimorphos post-impact orbit

Solution 516

Jan 18, 2023

Shantanu P. Naidu, Steven R. Chesley
Jet Propulsion Laboratory, California Institute of Technology

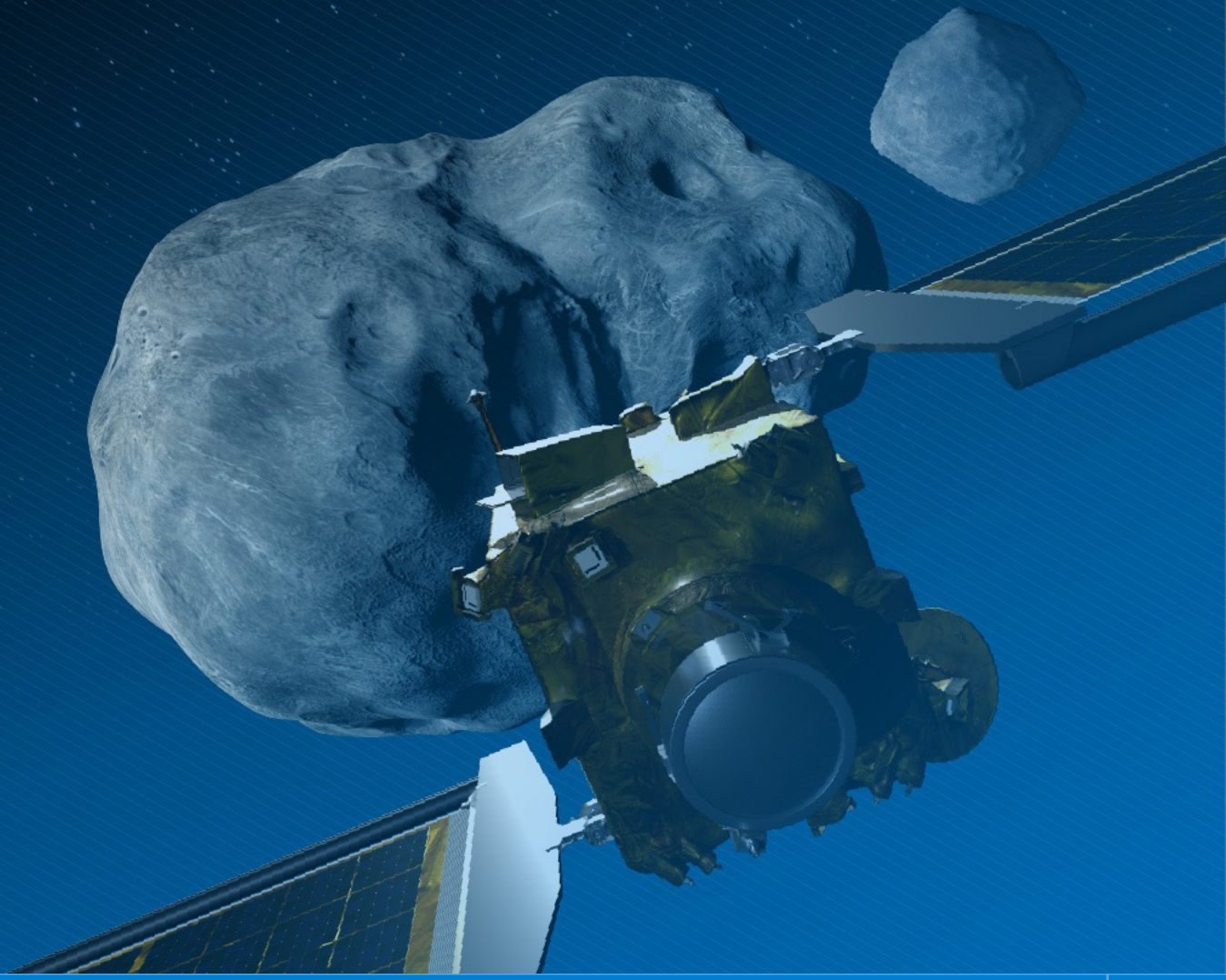

New post-impact dynamical model

- Pre-impact orbit is still characterized by $\boldsymbol{\lambda}$, $\boldsymbol{\beta}$, a, M_0, n_0, and $\dot{n}$.
- Post-impact orbit is now characterized by parameters ΔV_T, $\Delta \mathrm{V_R}$ and J_2.
- ΔV_T and $\Delta \mathrm{V_R}$ are transverse and radial components of the change in the velocity of Dimorphos due to the DART impact.
- J_2 is the oblateness parameter of Didymos.
- Position of Dimorphos remains unchanged at the instant of impact.
- We included the secular effects of J2 on the post-impact mean-motion and orbital precession.
- We estimated all 9 parameters.

Data

- 63 pre-impact mutual event times.
- 106 post-impact mutual event times (≤ 2022-Dec-31).
- 16 pre-impact OPNAV measurements. (unchanged from s504)
- 10 post-impact radar delay (unchanged from s504).
- 12 post-impact Doppler measurements (unchanged from s504).

Orbit parameters vs. J2

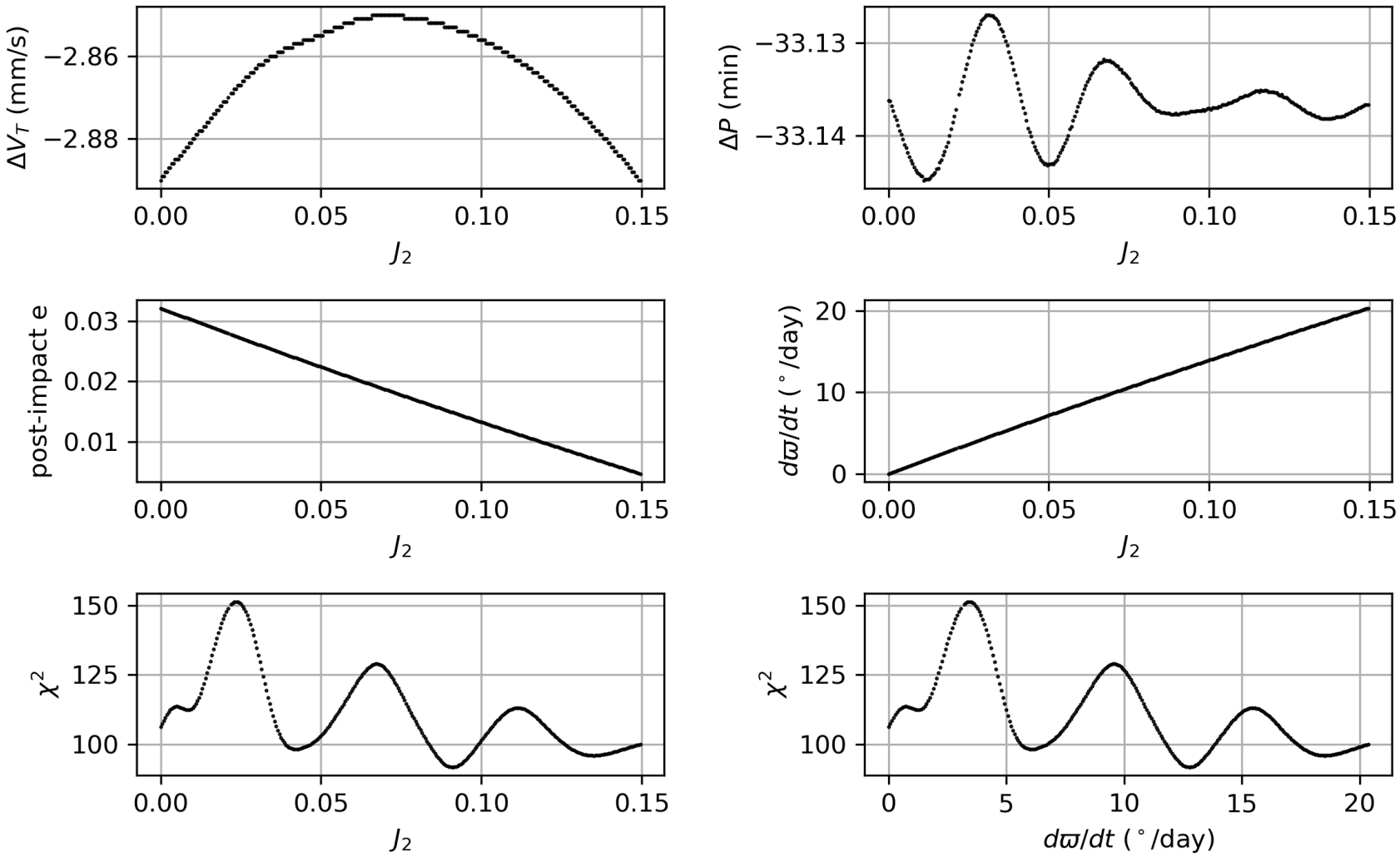

Residuals

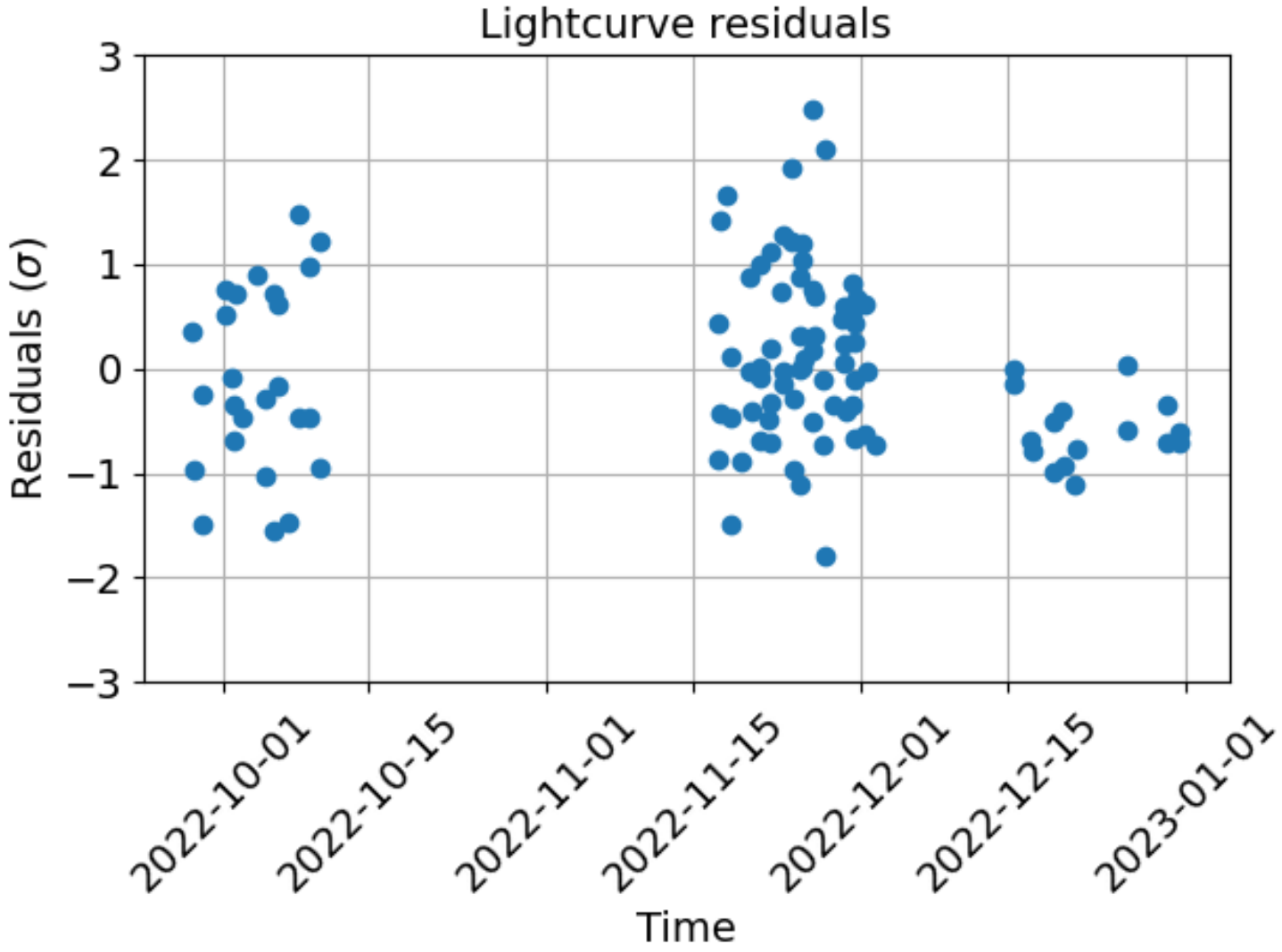
Lightcurve residuals
Residuals (σ)
3
2
1
0
−1
−2
−3
2022-10-01
2022-10-15
2022-11-01
2022-11-15
2022-12-01
2022-12-15
2023-01-01
Time

Solution 516 at epoch 2022 Sep 26 23:14:24.183 UTC

Parameter	Estimate +/- 1σ uncertainties
Orbit pole longitude (λ, degrees)	311.4 +/- 2.4
Orbit pole latitude (β, degrees)	-79.3 +/- 0.5
Pre-impact semimajor axis (a, km)	1.219 +/- 0.015
Mean anomaly at epoch (M_0, degrees)	175.8 +/- 2.4
Pre-impact period (h)	11.921489 +/- 0.000018
Mean motion at epoch (n_0, rad/sec)	(1.4640194 +/- 0.0000022) x 10^{-4}
Rate of change of mean motion ($\dot{n}$, rad/sec^2)	(4.9 +/- 0.7) x 10^{-18}
ΔV_R (mm/s)	0.3 +/- 0.2
ΔV_T (mm/s)	-2.85 +/- 0.04
J_2	0.090 +/- 0.004
Derived parameters	
Post-impact period (h)	11.3691 +/- 0.0003
Period change (min)	-33.14 +/- 0.02
Post-impact eccentricity	0.0151 +/- 0.0006
Post-impact argument of pericenter (ω_0^+, degrees)	2.5 +/- 5
Post-impact mean anomaly (M_0^+, degrees)	173 +/- 4
$\omega_0^+ + M_0^+$ (degrees)	175.6 +/- 2.4
$d\varpi/dt$ (degrees/day)	12.7 +/- 0.4
GM_{sys} (m^3/s^2)	38.19 +/- 1.5

Full precision GM_{sys} = 38.18918121621390159 62 m^3/s^2

Poorly characterized systematic errors can lead to 3x increase over the formal errors.

Delivery

- https://ssd.jpl.nasa.gov/ftp/eph/small_bodies/dart/dimorphos/
- SPK file: ‘dimorphos_s516.bsp’
  - Contains pre-impact as well as post-impact trajectories.
  - This SPK file avoids discontinuity between the pre- and post-impact orbits by computing post-impact elements based on the DART impact velocity vector and the estimated period change.
- There are two PCK files that describe the orientation of Dimorphos:
  - ‘dimorphos_s516-preimpact.tpc’: Valid for times prior to the DART impact at 2022 SEP 26 23:14:24.183 UTC
  - ‘dimorphos_s516-postimpact.tpc’: Valid for times after the DART impact at 2022 SEP 26 23:14:24.183 UTC

Post-impact lightcurve residuals

Time (one-way light-time corrected UTC)	Event type	Sigma (days)	Residuals (Sigma)
2022 SEP 28 04:28:07	Beginning of secondary eclipse	0.011	0.3497
2022 SEP 28 05:14:03	End of secondary eclipse	0.008	-0.9631
2022 SEP 29 03:02:00	Beginning of secondary eclipse	0.01	-0.2438
2022 SEP 29 03:39:53	End of secondary eclipse	0.0135	-1.4827
2022 OCT 01 06:11:57	Beginning of primary eclipse	0.0075	0.509
2022 OCT 01 06:45:04	End of primary eclipse	0.008	0.7625
2022 OCT 01 23:12:54	Beginning of secondary eclipse	0.0115	-0.0765
2022 OCT 02 00:08:03	End of secondary eclipse	0.0115	-0.6806
2022 OCT 02 04:43:58	Beginning of primary eclipse	0.0075	-0.3503
2022 OCT 02 05:28:45	End of primary eclipse	0.01	0.7137
2022 OCT 02 22:57:47	End of secondary eclipse	0.0075	-0.458
2022 OCT 04 08:13:37	Beginning of secondary eclipse	0.01	0.8989
2022 OCT 05 00:40:10	Beginning of primary eclipse	0.0085	-1.0339
2022 OCT 05 01:22:30	End of primary eclipse	0.008	-0.286
2022 OCT 05 23:39:33	Beginning of primary eclipse	0.0045	0.7216
2022 OCT 05 23:56:15	End of primary eclipse	0.0055	-1.5505
2022 OCT 06 05:29:36	Beginning of secondary eclipse	0.005	0.6191
2022 OCT 06 06:32:15	End of secondary eclipse	0.0055	-0.1643
2022 OCT 07 04:55:12	End of secondary eclipse	0.01	-1.4629
2022 OCT 08 08:34:39	Beginning of primary eclipse	0.0065	1.4864
2022 OCT 08 08:51:21	End of primary eclipse	0.007	-0.4609
2022 OCT 09 07:12:25	Beginning of primary eclipse	0.0065	0.9699
2022 OCT 09 07:33:35	End of primary eclipse	0.0085	-0.4586
2022 OCT 10 05:54:48	Beginning of primary eclipse	0.005	1.2157
2022 OCT 10 06:14:58	End of primary eclipse	0.0055	-0.9523

Post-impact lightcurve residuals

Time (one-way light-time corrected UTC)	Event type	Sigma (days)	Residuals (Sigma)
2022 NOV 17 07:42:48	Beginning of secondary eclipse	0.0035	0.4455
2022 NOV 17 08:52:56	End of secondary eclipse	0.003	-0.8622
2022 NOV 17 11:58:50	Beginning of primary occultation	0.0075	1.4166
2022 NOV 17 12:34:16	End of primary occultation	0.005	-0.4361
2022 NOV 18 04:42:40	Beginning of secondary occultation	0.0065	1.6543
2022 NOV 18 11:16:30	End of primary occultation	0.0055	-0.4743
2022 NOV 18 12:04:10	Beginning of primary eclipse	0.006	0.1193
2022 NOV 18 12:33:15	End of primary eclipse	0.0125	-1.4906
2022 NOV 19 11:25:43	End of primary eclipse	0.013	-0.8827
2022 NOV 20 08:13:46	Beginning of primary occultation	0.016	0.8724
2022 NOV 20 08:45:53	End of primary occultation	0.013	-0.0174
2022 NOV 20 10:13:43	End of primary eclipse	0.0185	-0.3989
2022 NOV 21 06:49:40	Beginning of primary occultation	0.0085	1.004
2022 NOV 21 07:28:33	End of primary occultation	0.007	-0.0805
2022 NOV 21 08:08:52	Beginning of primary eclipse	0.0065	0.0121
2022 NOV 21 08:57:33	End of primary eclipse	0.009	-0.6856
2022 NOV 22 02:26:26	End of secondary eclipse	0.007	-0.4852
2022 NOV 22 05:36:40	Beginning of primary occultation	0.0095	1.1235
2022 NOV 22 06:15:07	End of primary occultation	0.009	0.1888
2022 NOV 22 06:48:23	Beginning of primary eclipse	0.005	-0.3256
2022 NOV 22 07:37:20	End of primary eclipse	0.011	-0.7068
2022 NOV 23 09:43:29	Beginning of secondary occultation	0.0075	0.7386
2022 NOV 23 10:50:26	End of secondary occultation	0.0055	1.2773
2022 NOV 23 11:21:24	Beginning of secondary eclipse	0.0055	-0.0244
2022 NOV 23 12:34:07	End of secondary eclipse	0.008	-0.1458

Post-impact lightcurve residuals

Time (one-way light-time corrected UTC)	Event type	Sigma (days)	Residuals (Sigma)
2022 NOV 24 08:50:47	Beginning of secondary occultation	0.011	1.9136
2022 NOV 24 09:35:16	End of secondary occultation	0.0065	1.2134
2022 NOV 24 10:01:12	Beginning of secondary eclipse	0.0025	-0.9666
2022 NOV 24 11:14:21	End of secondary eclipse	0.0105	-0.2877
2022 NOV 25 01:50:35	Beginning of primary occultation	0.013	0.8736
2022 NOV 25 02:26:26	End of primary occultation	0.0065	0.3068
2022 NOV 25 02:57:15	Beginning of primary eclipse	0.0045	-0.0137
2022 NOV 25 03:39:18	End of primary eclipse	0.01	-1.1128
2022 NOV 25 07:16:36	Beginning of secondary occultation	0.0075	1.0391
2022 NOV 25 08:18:31	End of secondary occultation	0.0065	1.1933
2022 NOV 25 08:47:45	Beginning of secondary eclipse	0.0045	0.0196
2022 NOV 25 10:03:12	End of secondary eclipse	0.012	0.1005
2022 NOV 26 06:08:12	Beginning of secondary occultation	0.005	2.4934
2022 NOV 26 06:58:53	End of secondary occultation	0.0075	0.7642
2022 NOV 26 07:32:09	Beginning of secondary eclipse	0.0065	0.1837
2022 NOV 26 08:37:58	End of secondary eclipse	0.0085	-0.5022
2022 NOV 26 11:49:20	Beginning of primary occultation	0.008	0.694
2022 NOV 26 12:32:41	End of primary occultation	0.007	0.3103
2022 NOV 27 06:12:14	Beginning of secondary eclipse	0.0055	-0.1096
2022 NOV 27 07:17:36	End of secondary eclipse	0.0085	-0.7339
2022 NOV 27 10:47:25	Beginning of primary occultation	0.007	2.096
2022 NOV 27 12:20:09	End of primary eclipse	0.0085	-1.7813
2022 NOV 28 06:07:11	End of secondary eclipse	0.0035	-0.3398
2022 NOV 29 02:12:46	Beginning of secondary occultation	0.0115	0.4831
2022 NOV 29 08:02:58	Beginning of primary occultation	0.0075	0.589

Post-impact lightcurve residuals

Time (one-way light-time corrected UTC)	Event type	Sigma (days)	Residuals (Sigma)
2022 NOV 29 08:43:52	End of primary occultation	0.0045	0.2439
2022 NOV 29 09:10:39	Beginning of primary eclipse	0.006	0.0589
2022 NOV 29 09:59:28	End of primary eclipse	0.015	-0.3961
2022 NOV 30 00:54:00	Beginning of secondary occultation	0.0055	0.5497
2022 NOV 30 01:50:18	End of secondary occultation	0.0065	0.8123
2022 NOV 30 02:17:13	Beginning of secondary eclipse	0.006	-0.3486
2022 NOV 30 06:50:06	Beginning of primary occultation	0.013	0.437
2022 NOV 30 07:29:08	End of primary occultation	0.0065	0.265
2022 NOV 30 07:52:27	Beginning of primary eclipse	0.0065	-0.104
2022 NOV 30 08:36:40	End of primary eclipse	0.015	-0.6766
2022 NOV 30 12:22:53	Beginning of secondary occultation	0.011	0.6811
2022 DEC 01 05:41:51	Beginning of primary occultation	0.0165	0.6112
2022 DEC 01 07:22:56	End of primary eclipse	0.013	-0.6272
2022 DEC 01 10:56:47	Beginning of secondary occultation	0.0115	-0.0187
2022 DEC 02 05:59:34	End of primary eclipse	0.018	-0.7183
2022 DEC 15 11:23:08	Beginning of primary eclipse	0.005	-0.0001
2022 DEC 15 12:17:16	End of primary eclipse	0.0175	-0.1551
2022 DEC 17 04:04:13	End of secondary eclipse	0.008	-0.6963
2022 DEC 17 09:35:08	End of primary eclipse	0.009	-0.794
2022 DEC 19 05:53:13	Beginning of primary eclipse	0.0135	-0.9861
2022 DEC 19 07:03:56	End of primary eclipse	0.008	-0.4992
2022 DEC 20 04:49:09	Beginning of primary eclipse	0.01	-0.3977
2022 DEC 20 05:41:51	End of primary eclipse	0.0075	-0.9317
2022 DEC 21 09:06:20	Beginning of secondary eclipse	0.012	-1.0997
2022 DEC 21 10:09:41	End of secondary eclipse	0.015	-0.7634

Post-impact lightcurve residuals

Time (one-way light-time corrected UTC)	Event type	Sigma (days)	Residuals (Sigma)
2022 DEC 26 08:35:13	Beginning of primary eclipse	0.009	0.0426
2022 DEC 26 09:22:45	End of primary eclipse	0.0085	-0.5895
2022 DEC 30 03:26:21	Beginning of primary eclipse	0.007	-0.3393
2022 DEC 30 04:17:45	End of primary eclipse	0.006	-0.7111
2022 DEC 31 07:45:50	Beginning of secondary eclipse	0.008	-0.7075
2022 DEC 31 08:44:44	End of secondary eclipse	0.005	-0.6064

Goldstone radar range post-fit residuals

Receive time (UTC)	Range (m)	Sigma (m)	Residuals (sigma)
2022 OCT 04 11:32:00	-825	150	-0.0586
2022 OCT 04 11:55:00	-900	150	-0.2392
2022 OCT 09 10:28:09	828.2	450	-0.2411
2022 OCT 09 10:38:09	965	450	0.0014
2022 OCT 09 10:48:09	942.2	450	-0.0931
2022 OCT 09 10:57:57	896	450	-0.2211
2022 OCT 09 11:37:46	908	450	-0.1183
2022 OCT 09 11:46:47	896	450	-0.0886
2022 OCT 09 11:56:47	896	450	-0.0099
2022 OCT 09 12:05:46	862	450	-0.0007

Range refers to the radar range of Dimorphos relative to Didymos.
Measurements were made in radar images taken on Oct 4 (Goldstone monostatic) and Oct 9 (Goldstone -> GBT bistatic).
Oct 9 data is de-weighted by 3x $(\approx \sqrt{8})$ to mitigate effects of correlated measurement errors

Goldstone radar Doppler post-fit residuals

Receive time (UTC)	Doppler (Hz)	Sigma (Hz)	Residuals (sigma)
2022 SEP 27 11:22:02	-3.0	2.0	0.0688
2022 SEP 27 11:49:09	-5.0	2.0	-0.2457
2022 SEP 28 10:23:24	-4.0	2.0	0.2132
2022 SEP 30 10:22:13	-6.0	2.0	-0.1848
2022 OCT 01 10:05:51	-2.5	2.0	-0.135
2022 OCT 02 11:04:28	5.0	2.0	-0.6311
2022 OCT 04 09:58:15	7.0	2.0	-0.2016
2022 OCT 06 12:44:16	-8.0	2.0	-0.0987
2022 OCT 06 12:57:45	-8.0	2.0	-0.2537
2022 OCT 12 09:37:43	8.0	2.0	-0.404
2022 OCT 12 10:26:49	9.0	2.0	0.1311
2022 OCT 13 09:44:09	7.0	2.0	-0.3262

Table shows X-band (8560 MHz) Doppler measurements of Dimorphos are relative to Didymos. Measurements were made in radar echo power spectra obtained at Goldstone.

DART OPNAV measurements

Time (TDB)	deltaRA (deg)	sigmaRA (deg)	resRA (sig)	deltaDEC (deg)	sigmaDEC (deg)	resDEC (sigma)
2022 SEP 26 23:12:07.417	-0.0514196	0.0038304	0.326	-0.0125218	0.0034673	-0.043
2022 SEP 26 23:12:14.157	-0.0534928	0.0039585	0.244	-0.0117131	0.0034132	0.32
2022 SEP 26 23:12:20.897	-0.055801	0.0040724	0.142	-0.0125985	0.0034639	0.193
2022 SEP 26 23:12:27.637	-0.0576213	0.004194	0.194	-0.0134683	0.0035253	0.083
2022 SEP 26 23:12:33.415	-0.0593477	0.0043055	0.226	-0.0143021	0.0035859	-0.025
2022 SEP 26 23:12:40.155	-0.0615916	0.0044643	0.244	-0.0140441	0.0035711	0.206
2022 SEP 26 23:12:46.895	-0.0641259	0.0046184	0.239	-0.0150902	0.0036472	0.083
2022 SEP 26 23:12:53.635	-0.0667637	0.0047804	0.258	-0.016572	0.003762	-0.136
2022 SEP 26 23:13:00.375	-0.069919	0.0049938	0.218	-0.0157601	0.0036996	0.277
2022 SEP 26 23:13:07.115	-0.0732115	0.005196	0.208	-0.0170424	0.0038	0.14
2022 SEP 26 23:13:13.855	-0.0766707	0.0054239	0.226	-0.0180365	0.0038846	0.104
2022 SEP 26 23:13:20.595	-0.0803118	0.0056719	0.275	-0.019363	0.004004	0.008
2022 SEP 26 23:13:27.335	-0.0849044	0.0059557	0.229	-0.0204015	0.0040924	0.013
2022 SEP 26 23:13:34.075	-0.0893027	0.0062723	0.296	-0.0214126	0.0041959	0.052
2022 SEP 26 23:13:40.815	-0.0948127	0.0066306	0.276	-0.0225141	0.0042994	0.102
2022 SEP 26 23:13:48.518	-0.102054	0.0070766	0.243	-0.0253911	0.0045736	-0.159

Covariance matrix

	λ	β	a	M_0	n_0	$\dot{n}$	ΔV_R	ΔV_T	J_2
λ	1.6978E-03	-3.4796E-05	2.8131E-05	1.5771E-03	-1.7912E-12	-5.5225E-21	-3.7388E-11	-7.7112E-11	7.4099E-06
β	-3.4796E-05	6.0477E-05	-7.8612E-05	-2.9868E-05	2.5228E-13	8.5442E-22	-2.4653E-11	1.8436E-10	-1.0359E-05
a	2.8131E-05	-7.8612E-05	2.3970E-04	1.1279E-05	-4.0978E-13	-1.2960E-21	1.4951E-10	-5.6285E-10	3.2624E-05
M_0	1.5771E-03	-2.9868E-05	1.1279E-05	1.6957E-03	5.9184E-13	1.1619E-21	2.0433E-10	-1.9979E-11	5.2637E-06
n_0	-1.7912E-12	2.5228E-13	-4.0978E-13	5.9184E-13	4.7669E-20	1.4769E-28	2.3000E-18	1.1450E-18	-5.4215E-14
$\dot{n}$	-5.5225E-21	8.5442E-22	-1.2960E-21	1.1619E-21	1.4769E-28	4.6518E-37	6.3966E-27	3.5605E-27	-1.7203E-22
ΔV_R	-3.7388E-11	-2.4653E-11	1.4951E-10	2.0433E-10	2.3000E-18	6.3966E-27	3.6385E-14	-4.1206E-16	-1.1753E-10
ΔV_T	-7.7112E-11	1.8436E-10	-5.6285E-10	-1.9979E-11	1.1450E-18	3.5605E-27	-4.1206E-16	1.3241E-15	-7.8175E-11
J_2	7.4099E-06	-1.0359E-05	3.2624E-05	5.2637E-06	-5.4215E-14	-1.7203E-22	-1.1753E-10	-7.8175E-11	1.2773E-05

Previous solution 504

Parameter	Estimate +/- 1σ uncertainties
Orbit pole longitude (λ, degrees)	**313.3 +/- 2.6**
Orbit pole latitude (β, degrees)	**-79.3 +/- 0.5**
Pre-impact semimajor axis (a, km)	**1.206 +/- 0.018**
Mean anomaly at epoch (M_0, degrees)	178.9 +/- 2.7
Pre-impact period (h)	11.921473 +/- 0.000022
Mean motion at epoch (n_0, rad/sec)	(1.4640214 +/- 0.0000027) x 10^{-4}
Rate of change of mean motion ($\dot{n}$, rad/sec^2)	(5.4 +/- 0.8) x 10^{-18}
Post-impact period (h)	**11.371 +/- 0.003**
Period change (min)	**-33.02 +/- 0.16**
Change in mean motion (Δn, rad/sec)	(7.09 +/- 0.04) x 10^{-6}
GM_{sys} (km^3/s^2)	37.6136247195060170031
Epoch (UTC)	2022 Sep 26 23:14:24.183

	λ	β	a	M_0	n_0	$\dot{n}$	Δn
λ	2.05107362e-03	-7.09013795E-05	-2.94487823E-05	1.92852633E-03	-2.06274374E-12	-6.50002880E-21	2.63899355e-11
β	-7.09013795e-05	8.12550689E-05	-9.83483315E-05	-3.18380357E-05	6.77133762E-13	2.10366606E-21	-7.84642585e-11
a	-2.94487823e-05	-9.83483315E-05	3.08195403E-04	-1.25915120E-04	-1.26778220E-12	-3.72757114E-21	1.77115437e-10
M_0	1.92852633e-03	-3.18380357E-05	-1.25915120E-04	2.27757910E-03	2.71002241E-12	6.92814270E-21	-5.36094549e-10
n_0	-2.06274374e-12	6.77133762E-13	-1.26778220E-12	2.71002241E-12	7.26131949E-20	2.18340068E-28	-5.78675460e-18
$\dot{n}$	-6.50002880e-21	2.10366606E-21	-3.72757114E-21	6.92814270E-21	2.18340068E-28	6.65480189E-37	-1.63323264e-26
Δn	2.63899355e-11	-7.84642585E-11	1.77115437E-10	-5.36094549E-10	-5.78675460E-18	-1.63323264E-26	1.23573971e-15

- Primary ellipsoidal semi-axes: 425 x 425 x 310 m.
- Estimated λ, β, a, M_0, n_0, $\dot{n}$, and Δn.
- Poorly characterized systematic errors can lead to 3x increase over the formal errors.